Sub-shot-noise interferometry with two mode quantum states

Quentin Marolleau, Charlie Leprince, Victor Gondret, Denis Boiron, Christoph I Westbrook

Sub-shot-noise interferometry with two mode quantum states

Quentin Marolleau, Charlie Leprince, Victor Gondret, Denis Boiron, and Christoph I. Westbrook
Université Paris-Saclay, Institut d'Optique Graduate School,
CNRS, Laboratoire Charles Fabry, 91127, Palaiseau, France
(Dated: July 27, 2023)

We study the feasibility of sub-shot-noise interferometry with imperfect detectors, starting from twin-Fock states and two mode squeezed vacuum states. We derive analytical expressions for the corresponding phase uncertainty. We find that one can achieve phase shift measurements below the standard quantum limit, as long as the losses are smaller than a given threshold, and that the measured phase is close enough to an optimal value. We provide our analytical formulae in a Python package, accessible online.

I. INTRODUCTION

The ability to map many physical quantities onto a phase shift makes interferometry both a crucial and generic technique in metrology. It is widely known that because of entanglement, some non-classical states can lead to improved phase resolution compared to their classical counterparts [1–4]. Given an experimental resource of N identical bosons, an attractive choice is to use NOON states $\frac{1}{\sqrt{2}}(|N,0\rangle + |0,N\rangle)$. Indeed NOON states lead to a "Heisenberg limited" phase uncertainty $\Delta\phi = \mathcal{O}(N^{-1})$ [5–7], known to be optimal [8, 9]. This is a much more advantageous scaling than the best phase sensitivity reachable with classical systems ($\Delta\phi = 1/\sqrt{N}$), provided by a coherent state, and usually called the *standard quantum limit* (SQL) or *shot noise*. Other authors have proposed the use of "twin Fock" (TF) states $|\mathrm{TF}\rangle = |N/2, N/2\rangle$ and have shown that they also can achieve $1/N$ scaling in phase sensitivity [10, 11].

Unfortunately, NOON states are extremely fragile and behave even worse than classical states when losses are present [12, 13]. In addition, they are very challenging to prepare, and their realization with N larger than a few units has not been achieved [14, 15].

The effect of loss in quantum enhanced interferometers has been studied more generally, and states minimizing the phase uncertainty in the presence of loss have been found [16–18]. These states can be expressed as superpositions of states of the form:

$$|N :: m\rangle_{\pm} = \frac{1}{\sqrt{2}}\left(|N-m, m\rangle \pm |m, N-m\rangle\right). \qquad (1)$$

Like NOON states, these states involve superpositions of strong population imbalances between the two modes (a NOON state is in fact the special case $m = 0$). This imbalance is responsible for the enhanced sensitivity, but these states can retain their coherence despite a loss of order m particles, and thus are more robust [19]. In the presence of losses however, even these states can only surpass the standard quantum limit by a numerical factor, meaning that $\Delta\phi = \mathcal{O}(N^{-1/2})$ is the best scaling possible [17, 20]. Here again, although the optimal states are conceptually interesting, their experimental realization is not presently realistic.

On the other hand, it is well known that the mixing on a beam splitter of the twin-Fock states mentioned above gives rise to a superposition of $|2n :: 2k\rangle_{\pm}$ states [21, 22], and one might wonder about the robustness of such a superposition in the presence of loss. A related state is the two-mode squeezed state (TMS) [23], which is a superposition of twin Fock states with different particle numbers. Both of these states are widely used and can be produced with a large number of particles [24–29]. These states are different from another type of experimentally realizable states, the "spin squeezed" states, see fig. 5 of [4].

Here we will analyse the performance of twin Fock and two-mode squeezed states in the presence of loss. Unlike for spin squeezed states, the relevant observable is not simply the population difference and in fact several choices are a priori possible. We will follow other authors in using the variance of the population difference as the interferometric observable [10, 11]. We find that the sensitivity in this case only differs from that of the optimal state by a numerical factor and that one can surpass the standard quantum limit if the losses are low enough.

II. OUR MODEL

We will consider the interferometer configuration represented in fig. 1, and for the sake of clarity we will distinguish the *input* state (before the first beam splitter) that one must prepare, from the *probe* state (after the first beam splitter) that exhibits some phase sensitivity. We assume that the losses are only caused by the detectors, having the same quantum efficiency η, and we will consider $\Delta\phi = 1/\sqrt{\eta N}$ to be the SQL, against which we should compare our results. Our input state is either a twin Fock state or a two-mode squeezed state. Note that without an initial beam splitter, these states produce interference patterns that are independent of the phase [21, 22, 30].

Two-mode squeezed states are well known in quantum optics, as they are spontaneously generated from vacuum with a quadratic interaction hamiltonian. By denoting $\xi = re^{i\theta}$ the squeezing parameter, whose norm r is proportional to the interaction time, such a state reads

$$|\mathrm{TMS}\rangle = \frac{1}{\cosh(r)} \sum_{n=0}^{\infty} e^{in\theta} \tanh^n(r)\, |n, n\rangle \qquad (2)$$

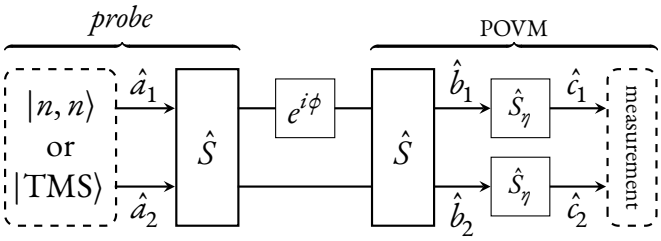

Figure 1. Generic diagram of an interferometry experiment, using a two-mode pure state at the input modes $(\hat{a}_1, \hat{a}_2)$ of the first beam splitter. After the generation of a probe state, a phase shift is applied, and the detection is performed with a POVM (positive operator valued measure). The 50:50 beam splitter, corresponding to the unitary operator $\hat{S}$ is applied twice, and the phase difference between the two arms is ϕ. The detectors have a finite quantum efficiency η, assumed to be equal, and is modelled with additional beam splitters $\hat{S}_\eta$ applied to the output modes of the interferometer $(\hat{b}_1, \hat{b}_2)$. The operators $\hat{c}_1$ and $\hat{c}_2$ represent the modes that are effectively detected.

in the Fock basis relative to the modes $\hat{a}_1$ and $\hat{a}_2$ (see fig. 1).

The action of the interferometer on the input state is described by the unitary operator $\hat{U}$:

$$\hat{U} = \hat{S}\begin{pmatrix} e^{i\phi} & 0 \\ 0 & 1 \end{pmatrix}\hat{S} = e^{i\frac{\phi}{2}}\begin{bmatrix} i\sin\left(\frac{\phi}{2}\right) & \cos\left(\frac{\phi}{2}\right) \\ -\cos\left(\frac{\phi}{2}\right) & -i\sin\left(\frac{\phi}{2}\right) \end{bmatrix} \tag{3}$$

The losses are modelled by additional beam splitters $\hat{S}_\eta$ placed at the output ports:

$$\hat{S}_\eta = \begin{bmatrix} \sqrt{\eta} & \sqrt{1-\eta} \\ -\sqrt{1-\eta} & \sqrt{\eta} \end{bmatrix} \tag{4}$$

With the input and output annihilation operators defined in fig. 1, we introduce the additional notations for the number operators:

$$\hat{N}_{\alpha_i} = \hat{\alpha}_i^\dagger \hat{\alpha}_i \quad / \quad \alpha \in \{a, b, c\}\ ,\ i \in \{1, 2\} \tag{5}$$

and the detected particle number difference at the output, with and without losses:

$$\begin{cases} \hat{D}_\eta = \dfrac{1}{2}\left(\hat{N}_{c_2} - \hat{N}_{c_1}\right) \\ \hat{D} = \dfrac{1}{2}\left(\hat{N}_{b_2} - \hat{N}_{b_1}\right) = \hat{D}_{\eta=1} \end{cases} \tag{6}$$

We also denote $N = \left\langle \hat{N}_{a_1} + \hat{N}_{a_2} \right\rangle = \left\langle \hat{N}_{b_1} + \hat{N}_{b_2} \right\rangle$ the average number of particles in the initial state. In the case of a twin Fock state $|n, n\rangle$, we simply have $N = 2n$, whereas for a two-mode squeezed state $N = 2\sinh^2(r)$, i.e. twice the average number of particles per mode. The mean number of detected particles therefore is ηN.

The operator $\hat{U}$ provides the expansion of $\hat{D}$ in terms of the input modes:

$$\hat{D} = \frac{1}{2}\left[\cos(\phi)\left(\hat{N}_{a_1} - \hat{N}_{a_2}\right) + i\sin(\phi)\left(\hat{a}_1^\dagger \hat{a}_2 - \hat{a}_2^\dagger \hat{a}_1\right)\right] \tag{7}$$

Therefore, whatever the phase ϕ and the quantum efficiency η, a twin Fock state placed at the input of the interferometer yields a vanishing expectation value for $\hat{D}$. Due to linearity, the same is true for two-mode squeezed states. This means that $\hat{D}$ itself is not a suitable observable to recover information about the phase ϕ with those states. However, following previous authors [10, 11], one can study $\hat{D}^2$ which characterizes the width of these distributions. Indeed, one can derive [31]:

$$\begin{cases} \left\langle \hat{D}_\eta^2 \right\rangle_{\mathrm{tf}} = \eta^2 \dfrac{N}{4}\left(1 + \dfrac{N}{2}\right)\sin^2(\phi) + \eta(1-\eta)\dfrac{N}{4} \\ \left\langle \hat{D}_\eta^2 \right\rangle_{\mathrm{tms}} = \eta^2 \dfrac{N}{2}\left(1 + \dfrac{N}{2}\right)\sin^2(\phi) + \eta(1-\eta)\dfrac{N}{4} \end{cases} \tag{8}$$

making explicit the phase dependence.

III. RESULTS

The phase uncertainty can be computed analytically using

$$\Delta\phi = \frac{\sqrt{\mathrm{Var}\left[\hat{D}_\eta^2\right]}}{\left|\dfrac{\partial}{\partial\phi}\left[\left\langle \hat{D}_\eta^2 \right\rangle\right]\right|}. \tag{9}$$

If the detectors are lossless ($\eta = 1$), the phase uncertainties are given by:

$$\begin{cases} \Delta\phi_{\mathrm{tf}} = \dfrac{1}{\cos(\phi)\sqrt{N(N+2)}}\sqrt{2 + \left(-3 + \frac{N}{4} + \frac{N^2}{8}\right)\sin^2(\phi)} \\ \Delta\phi_{\mathrm{tms}} = \dfrac{1}{\cos(\phi)\sqrt{N(N+2)}}\sqrt{1 + 2N(N+2)\sin^2(\phi)} \end{cases} \tag{10}$$

In the neighbourhood of $\phi = 0$, we find Heisenberg limited scaling $\Delta\phi = \mathcal{O}(N^{-1})$.

When we include losses, the analogous expressions become rather long and we leave them to the supplemental materials [31]. As an example, in fig. 2 we show that the phase uncertainty $\Delta\phi$ can be smaller than the standard quantum limit. In addition, the phase uncertainty has a minimum at a non-zero phase ϕ_0 which depends on the detection efficiency, number of particles and the input state (see fig. 3). The optimal phase is shifted due to a divergence at zero phase in eq. (9): $\Delta\phi \underset{\phi=0}{=} \mathcal{O}(\phi^{-1})$. This type of profile has been observed experimentally [32]. From the study of the variations of $\Delta\phi$ as a function of ϕ, one can compute the optimal phase ϕ_0 around which an experiment should operate to perform precision measurements. This means that during an experiment, one must be able to tune a phase offset, for instance in optics by adding a tiltable glass plate.

In fig. 3 we show color maps of the values of ϕ_0 as a function of the number of particles N and the quantum efficiency η. Regions where sub-shot-noise measurements are possible correspond to non-hashed regions. It appears in these maps that this question is mostly related

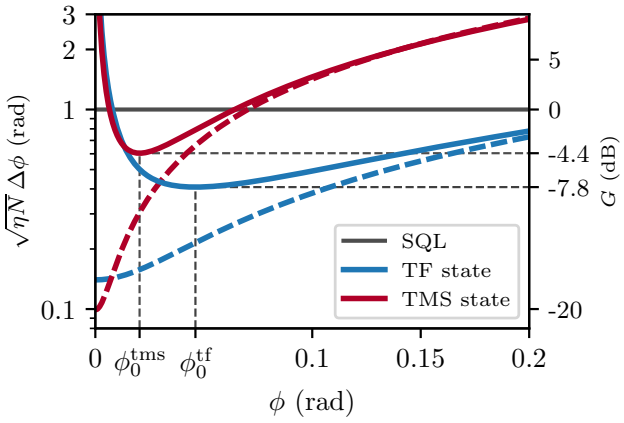

Figure 2. Ratio between the phase uncertainty $\Delta\phi$ and the SQL, using respectively twin-Fock state (in blue) and two-mode squeezed state (in red) as input states of the interferometer. The dashed lines correspond to the situation where the quantum efficiency of the detectors is assumed to be perfect ($\eta = 1$), whereas the plain lines refer to detectors with finite quantum efficiency (here $\eta = 0.95$). Both types of states have an average population of 100 particles (50 per mode). We also give the gain in decibel defined as $G = 20\log\left(\sqrt{\eta N}\,\Delta\phi\right)$.

to the quantum efficiency of the detectors: depending on whether one is dealing with twin Fock or two-mode squeezed states, a threshold of $\eta \approx 0.7$ or respectively $\eta \approx 0.9$ must be achieved to surpass the SQL.

We have computed $\Delta\phi_0$ [31], the phase uncertainty when the measurement is performed at the optimal phase ϕ_0. When N is small, $\Delta\phi_0$ varies similarly to a power law $\Delta\phi_0 \approx 1/N^\alpha$ with $0.5 < \alpha < 1$, depending on the value of η (an example is plotted in fig. 4). Experimentally, in this region one obtains significant gains with respect to the standard quantum limit by increasing the number of particles. In the asymptotic region, where N goes to infinity, we recover the $\Delta\phi_0 = \mathcal{O}(N^{-1/2})$ scaling [17, 20].

We also computed

$$\gamma(\eta) = \lim_{N\to\infty} \sqrt{\eta N}\,\Delta\phi_0 \tag{11}$$

which is the ratio between $\Delta\phi_0$ and the standard quantum limit, in the asymptotic limit. This quantity tells what value of η must be reached to go below the SQL. It has been proven [17] that

$$\sqrt{\eta N}\,\Delta\phi \geq \sqrt{1-\eta} \tag{12}$$

but this bound is tight only when using optimal input states, as well as an observable which is not explicitly known. In our case, the function γ is actually a simple dilation of the lower bound (12) (see fig. 5):

$$\begin{cases} \gamma^{\rm tf}(\eta) = \sqrt{3}\sqrt{1-\eta} \\ \gamma^{\rm tms}(\eta) = \underbrace{\left(\frac{2}{5}\right)^{1/4}\sqrt{5+2\sqrt{10}}}_{\approx 2.676}\sqrt{1-\eta} \end{cases} \tag{13}$$

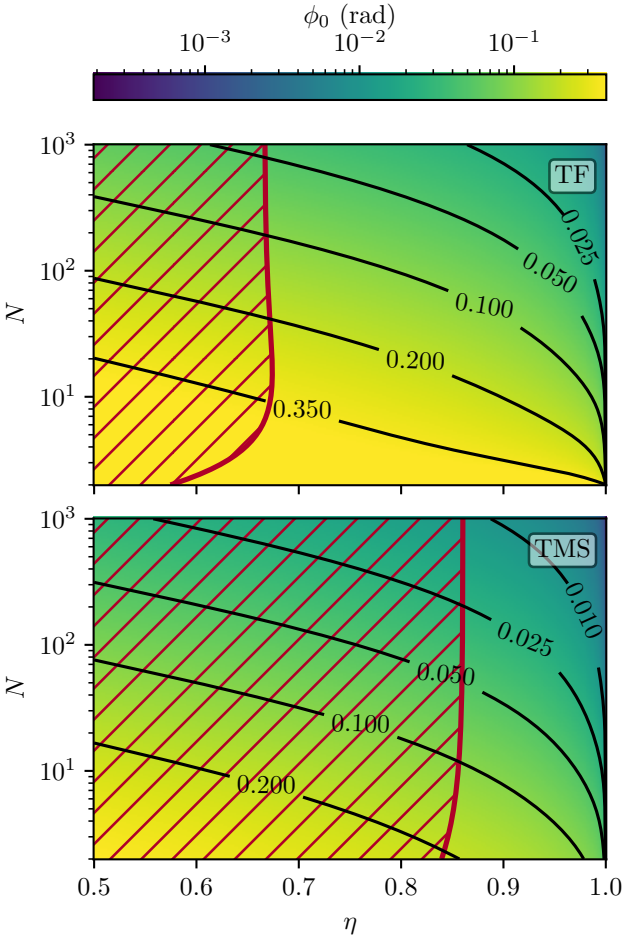

Figure 3. Optimal phase ϕ_0 that minimises the phase uncertainty during a measurement, plotted as a function of the number of particles in the interferometer N and the quantum efficiency of the detectors η. The red hatches exhibit the subdomain of the (η, N) plane where no measurement below SQL can be performed. Isolines of ϕ_0 are plotted in black. The top graph represents ϕ_0 for the TF state, while the bottom graph refers to the TMS state.

Our simple measurement protocol is therefore similar to an optimal situation where ideal states are used.

IV. CONCLUSION

The chief conclusion of this work is that when accounting for non-unit quantum efficiency, there exist experimentally accessible states which can achieve phase sensitivity close to the theoretical limit. As in other schemes to surpass the standard quantum limit, the quantum efficiency of the detectors is critical. With TF states, a 95% quantum efficiency results in a 8 dB improvement compared to the SQL, which is not very far from the theoretical bound of 13 dB given by eq. (12). For a TMS the gain is only 4.4 dB. Still, we expect that such improvement factors could be useful in some interferometers

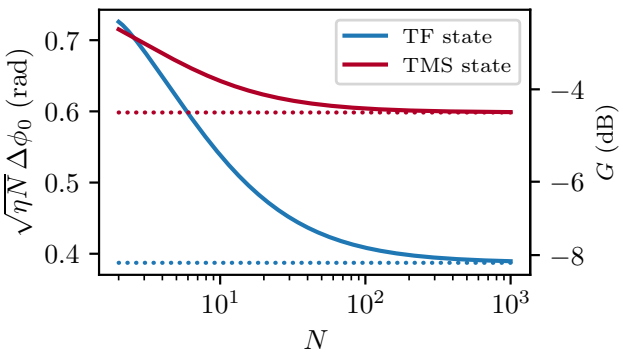

Figure 4. Asymptotic behaviour of the ratio between the phase uncertainty $\Delta\phi_0$ (i.e. $\Delta\phi$ estimated at the optimal phase ϕ_0) and the SQL, as a function of the number of particles, for both TF and TMS states. The quantum efficiency is set to $\eta = 0.95$. Contrary to the lossless detectors case that provides a $\frac{1}{N}$ Heisenberg limited scaling, the ratios converge towards a finite limit (dotted line), meaning that the SQL is surpassed only by a constant factor. We also give the gain in decibel defined as $G = 20\log\left(\sqrt{\eta N}\,\Delta\phi_0\right)$.

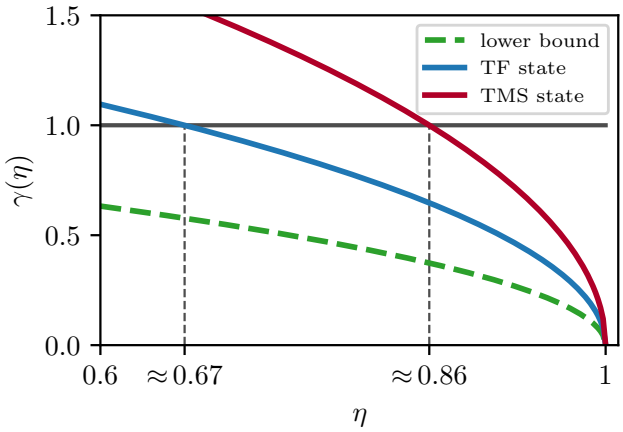

Figure 5. Ratio between the phase uncertainty $\Delta\phi_0$ and the SQL, in the asymptotic regime, as a function of the quantum efficiency (cf. eq. (11)). We find that both TF and TMS states give a profile which is proportional to the one obtained with an optimized input state (green dashed line, cf. eq. (12)). We also see in this graph the minimal values of η leading to sub-shot-noise measurements (these values correspond to the limit $N \to \infty$ of the red lines in fig. 3).

where increasing the number of particles to reduce the shot noise is not practical. Whether twin Fock or two-mode squeezed states constitute a real advantage compared to spin squeezing will require more work in the future using comparisons in realistic experimental situations [4]. The fact that these relatively accessible states are not far from the optimized ones is an encouraging sign.

Our analytical formulae are provided in the supplementary materials and are implemented in a Python package, accessible online at `https://github.com/quentinmarolleau/qsipy`.

ACKNOWLEDGMENTS

The research leading to these results has received funding from QuantERA Grant No. ANR-22-QUA2-0008-01 (MENTA) and ANR Grant No. 20-CE-47-0001-01 (COSQUA), the LabEx PALM, Région Ile-de-France in the framework of the DIM SIRTEQ program and Quantum-Saclay.

[1] V. Giovannetti, S. Lloyd, and L. Maccone, Quantum-Enhanced Measurements: Beating the Standard Quantum Limit, Science **306**, 1330 (2004).
[2] V. Giovannetti, S. Lloyd, and L. Maccone, Quantum Metrology, Physical Review Letters **96**, 010401 (2006).
[3] L. Pezzé and A. Smerzi, Entanglement, Nonlinear Dynamics, and the Heisenberg Limit, Physical Review Letters **102**, 100401 (2009).
[4] L. Pezzè, A. Smerzi, M. K. Oberthaler, R. Schmied, and P. Treutlein, Quantum metrology with nonclassical states of atomic ensembles, Reviews of Modern Physics **90**, 035005 (2018).
[5] J. J. . Bollinger, W. M. Itano, D. J. Wineland, and D. J. Heinzen, Optimal frequency measurements with maximally correlated states, Physical Review A **54**, R4649 (1996).
[6] J. P. Dowling, Correlated input-port, matter-wave interferometer: Quantum-noise limits to the atom-laser gyroscope, Physical Review A **57**, 4736 (1998).
[7] V. Giovannetti, S. Lloyd, and L. Maccone, Advances in

quantum metrology, Nature Photonics **5**, 222 (2011).
[8] W. Heitler, *The Quantum Theory of Radiation*, 3rd ed., Dover Books on Physics (Dover Publications, New York, 1954) p. 65.
[9] Z. Y. Ou, Fundamental quantum limit in precision phase measurement, Physical Review A **55**, 2598 (1997).
[10] M. J. Holland and K. Burnett, Interferometric detection of optical phase shifts at the Heisenberg limit, Physical Review Letters **71**, 1355 (1993).
[11] P. Bouyer and M. A. Kasevich, Heisenberg-limited spectroscopy with degenerate Bose-Einstein gases, Physical Review A **56**, R1083 (1997).
[12] J. A. Dunningham, K. Burnett, and S. M. Barnett, Interferometry below the Standard Quantum Limit with Bose-Einstein Condensates, Physical Review Letters **89**, 150401 (2002).
[13] U. Dorner, R. Demkowicz-Dobrzanski, B. J. Smith, J. S. Lundeen, W. Wasilewski, K. Banaszek, and I. A. Walmsley, Optimal Quantum Phase Estimation, Physical Review Letters **102**, 040403 (2009).
[14] T. Nagata, R. Okamoto, J. L. O'Brien, K. Sasaki, and S. Takeuchi, Beating the Standard Quantum Limit with Four-Entangled Photons, Science **316**, 726 (2007).
[15] I. Afek, O. Ambar, and Y. Silberberg, High-NOON States by Mixing Quantum and Classical Light, Science **328**, 879 (2010).
[16] R. Demkowicz-Dobrzanski, U. Dorner, B. J. Smith, J. S. Lundeen, W. Wasilewski, K. Banaszek, and I. A. Walmsley, Quantum phase estimation with lossy interferometers, Physical Review A **80**, 013825 (2009).
[17] J. Kołodyński and R. Demkowicz-Dobrzański, Phase estimation without *a priori* phase knowledge in the presence of loss, Physical Review A **82**, 053804 (2010).
[18] S. Knysh, V. N. Smelyanskiy, and G. A. Durkin, Scaling laws for precision in quantum interferometry and the bifurcation landscape of the optimal state, Physical Review A **83**, 021804(R) (2011).
[19] S. D. Huver, C. F. Wildfeuer, and J. P. Dowling, Entangled Fock states for robust quantum optical metrology, imaging, and sensing, Physical Review A **78**, 063828 (2008).
[20] B. M. Escher, R. L. de Matos Filho, and L. Davidovich, General framework for estimating the ultimate precision limit in noisy quantum-enhanced metrology, Nature Physics **7**, 406 (2011).
[21] R. A. Campos, B. E. A. Saleh, and M. C. Teich, Quantum-mechanical lossless beam splitter: SU(2) symmetry and photon statistics, Physical Review A **40**, 1371 (1989).
[22] K. Yu Spasibko, F. Töppel, T. Sh Iskhakov, M. Stobińska, M. V. Chekhova, and G. Leuchs, Interference of macroscopic beams on a beam splitter: Phase uncertainty converted into photon-number uncertainty, New Journal of Physics **16**, 013025 (2014).
[23] P. M. Anisimov, G. M. Raterman, A. Chiruvelli, W. N. Plick, S. D. Huver, H. Lee, and J. P. Dowling, Quantum Metrology with Two-Mode Squeezed Vacuum: Parity Detection Beats the Heisenberg Limit, Physical Review Letters **104**, 103602 (2010).
[24] X.-Y. Luo, Y.-Q. Zou, L.-N. Wu, Q. Liu, M.-F. Han, M. K. Tey, and L. You, Deterministic entanglement generation from driving through quantum phase transitions, Science **355**, 620 (2017).
[25] X. Deng, S. Li, Z.-J. Chen, Z. Ni, Y. Cai, J. Mai, L. Zhang, P. Zheng, H. Yu, C.-L. Zou, S. Liu, F. Yan, Y. Xu, and D. Yu, Heisenberg-limited quantum metrology using 100-photon fock states (2023), arXiv:2306.16919 [quant-ph].
[26] F. Anders, A. Idel, P. Feldmann, D. Bondarenko, S. Loriani, K. Lange, J. Peise, M. Gersemann, B. Meyer-Hoppe, S. Abend, N. Gaaloul, C. Schubert, D. Schlippert, L. Santos, E. Rasel, and C. Klempt, Momentum Entanglement for Atom Interferometry, Physical Review Letters **127**, 140402 (2021).
[27] E. M. Bookjans, C. D. Hamley, and M. S. Chapman, Strong Quantum Spin Correlations Observed in Atomic Spin Mixing, Physical Review Letters **107**, 210406 (2011).
[28] T. Sh Iskhakov, K. Yu Spasibko, M. V. Chekhova, and G. Leuchs, Macroscopic Hong–Ou–Mandel interference, New Journal of Physics **15**, 093036 (2013).
[29] G. Harder, T. J. Bartley, A. E. Lita, S. W. Nam, T. Gerrits, and C. Silberhorn, Single-Mode Parametric-Down-Conversion States with 50 Photons as a Source for Mesoscopic Quantum Optics, Physical Review Letters **116**, 143601 (2016).
[30] C. K. Hong, Z. Y. Ou, and L. Mandel, Measurement of subpicosecond time intervals between two photons by interference, Physical Review Letters **59**, 2044 (1987).
[31] See Supplemental Material at [URL will be inserted by publisher] for more details about the results taking into account the finite quantum efficiency, and their derivation.
[32] B. Lücke, M. Scherer, J. Kruse, L. Pezzé, F. Deuretzbacher, P. Hyllus, O. Topic, J. Peise, W. Ertmer, J. Arlt, L. Santos, A. Smerzi, and C. Klempt, Twin Matter Waves for Interferometry Beyond the Classical Limit, Science **334**, 773 (2011).

Supplemental material for
Sub-shot-noise interferometry with two mode quantum states

Quentin Marolleau, Charlie Leprince, Victor Gondret, Denis Boiron, and Christoph I. Westbrook
Université Paris-Saclay, Institut d'Optique Graduate School,
CNRS, Laboratoire Charles Fabry, 91127, Palaiseau, France

(Dated: July 27, 2023)

CONTENTS

FOREWORD ON THE PYTHON PACKAGE: `QSIPY`

We provide a Python package that implements all the formulae that we present in the main article and this supplemental material. The source code is distributed under the MIT licence and can be accessed on GitHub: `https://github.com/quentinmarolleau/qsipy`.

The package itself is also built and published in the official Python Package Index (PyPI), under the name `qsipy`. The interested reader may install it on its own Python environment by simply using the `pip` package manager:

```
pip install qsipy
```

Figures of the article are generated using the version `v1.0.0` of `qsipy`, the source code generating those is also available online.

I. PARAMETRIZATION OF THE PROBLEM

I.1. Operator definitions

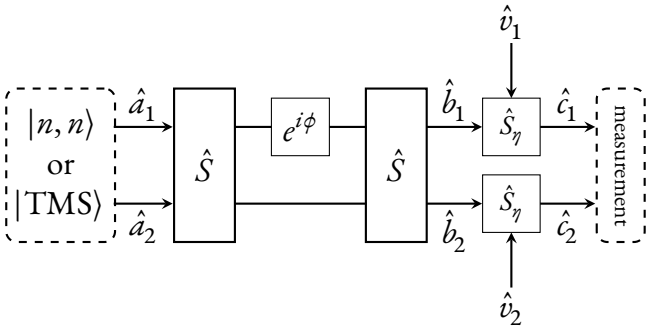

Figure S1. Scheme of the interferometer that we study. $\hat{a}_1$ and $\hat{a}_2$ are the input modes, 50:50 beam splitters, corresponding to the unitary operator $\hat{S}$ are applied twice, and the phase difference between the two arms is ϕ. The detectors placed at the output ports have a finite quantum efficiency η, assumed to be equal, and that is modelled with additional beam splitters $\hat{S}_\eta$ applied to the output modes of the interferometer $(\hat{b}_1, \hat{b}_2)$. The operators $\hat{c}_1$ and $\hat{c}_2$ represent the modes that are effectively detected. The modes $\hat{v}_1$ and $\hat{v}_2$ represent the vacuum channels.

Following the notation of fig. S1, we denote N the average value of the total number of atoms in the interferometer:

$$N \triangleq \left\langle \hat{N}_{a_1} + \hat{N}_{a_2} \right\rangle = \left\langle \hat{N}_{b_1} + \hat{N}_{b_2} \right\rangle \tag{1}$$

We have

$$\hat{S} = \frac{1}{\sqrt{2}} \begin{pmatrix} 1 & 1 \\ -1 & 1 \end{pmatrix} \tag{2}$$

corresponding to the special case of the beam splitter that does not apply any phase shift. Without loss of generality we chose the beam splitters to be real matrix because the observable that we consider are only sensitive to the actual phase difference between the two arms of the interferometer.

$$\hat{\Phi} = \begin{pmatrix} e^{i\phi} & 0 \\ 0 & 1 \end{pmatrix} \tag{3}$$

$$\hat{U} = \hat{S}\hat{\Phi}\hat{S} = e^{i\frac{\phi}{2}} \begin{pmatrix} i\sin\left(\frac{\phi}{2}\right) & \cos\left(\frac{\phi}{2}\right) \\ -\cos\left(\frac{\phi}{2}\right) & -i\sin\left(\frac{\phi}{2}\right) \end{pmatrix} \tag{4}$$

$$\begin{pmatrix} \hat{b}_1 \\ \hat{b}_2 \end{pmatrix} = \hat{U} \begin{pmatrix} \hat{a}_1 \\ \hat{a}_2 \end{pmatrix} \tag{5}$$

We also have the beam splitters modelling the losses:

$$\hat{S}_\eta = \begin{pmatrix} \sqrt{\eta} & \sqrt{1-\eta} \\ -\sqrt{1-\eta} & \sqrt{\eta} \end{pmatrix} \tag{6}$$

such that

$$\hat{c}_i = \sqrt{\eta}\,\hat{b}_i + \sqrt{1-\eta}\,\hat{v}_i \quad / \quad i \in \{1,2\} \tag{7}$$

We finally introduce notations for the number operators:

$$\hat{N}_{\alpha_i} = \hat{\alpha}_i^\dagger \hat{\alpha}_i \quad / \quad \alpha \in \{a,b,c\}\ ,\ i \in \{1,2\} \tag{8}$$

input spin operators:

$$\begin{cases} \hat{J}_x = \frac{1}{2}\left(\hat{a}_1^\dagger \hat{a}_2 + \hat{a}_2^\dagger \hat{a}_1\right) \\ \hat{J}_y = \frac{1}{2i}\left(\hat{a}_1^\dagger \hat{a}_2 - \hat{a}_2^\dagger \hat{a}_1\right) \\ \hat{J}_z = \frac{1}{2}\left(\hat{N}_{a_1} - \hat{N}_{a_2}\right) \end{cases} \tag{9}$$

and the observables of interest:

$$\begin{cases} \hat{D}_\eta = \dfrac{1}{2}\left(\hat{N}_{c_2} - \hat{N}_{c_1}\right) \\ \hat{D} = \dfrac{1}{2}\left(\hat{N}_{b_2} - \hat{N}_{b_1}\right) = \hat{D}_{\eta=1} \end{cases} \tag{10}$$

I.2. Two-mode squeezed vacuum state and preliminary results

We remind the definition of a two-mode squeezed vacuum (TMS) state, with average total population N:

$$|\mathrm{TMS}\rangle \triangleq \sqrt{\frac{2}{2+N}} \sum_{n=0}^{\infty} \left(\frac{N}{2+N}\right)^{\frac{n}{2}} |n,n\rangle \tag{11}$$

in order to keep compact notations during the calculations, we will often use the *thermal weight*:

$$P_{th}(n) = \frac{2}{2+N}\left(\frac{N}{2+N}\right)^n \tag{12}$$

corresponding to the probability to measure n particles in a given mode of the TMS state.

We also highlight the fact that

$$\hat{J}_z\,|n,n\rangle = \hat{J}_z\,|\mathrm{TMS}\rangle = 0 \tag{13}$$

and finally:

$$\left\langle \hat{J}_x \right\rangle = \left\langle \hat{J}_y \right\rangle = 0 \tag{14}$$

for both twin Fock and two-mode squeezed vacuum states.

II. EXPANSION OF $\hat{D}$, $\hat{D}^2$, $\hat{D}_\eta$ AND $\hat{D}_\eta^2$

$$\hat{D} = \cos(\phi)\hat{J}_z - \sin(\phi)\hat{J}_y \tag{15}$$

$$\hat{D}^2 = \cos^2(\phi)\hat{J}_z^2 + \sin^2(\phi)\hat{J}_y^2 - 2\sin(\phi)\cos(\phi)\hat{J}_y\hat{J}_z + i\sin(\phi)\cos(\phi)\hat{J}_x \tag{16}$$

Since there is no particle in the vacuum channels for the input state, we always have $\hat{v}_i \left|\psi\right\rangle_{\text{input}} = 0$. For a sake of simplicity, we reduce the writing of $\hat{D}_\eta$ and $\hat{D}_\eta^2$ to the terms giving a non zero contribution. This means that (for either $\hat{D}_\eta$ and $\hat{D}_\eta^2$) we drop all the terms containing $\hat{v}_{i\in\{1,2\}}$ annihilation operators on their rightmost side:

$$\hat{D}_\eta = \eta\hat{D} + \frac{1}{2}\sqrt{\eta(1-\eta)}\left(\hat{v}_2^\dagger\,\hat{b}_2 - \hat{v}_1^\dagger\,\hat{b}_1\right) \tag{17}$$

$$\begin{aligned}\hat{D}_\eta^2 = \eta^2\hat{D}^2 &+ \frac{\eta(1-\eta)}{4}\left[(\hat{v}_1^\dagger)^2\,\hat{b}_1^2 + (\hat{v}_2^\dagger)^2\,\hat{b}_2^2 + \hat{N}_{b_1} + \hat{N}_{b_2} - 2\,\hat{b}_1\hat{b}_2\,\hat{v}_1^\dagger\hat{v}_2^\dagger\right]\\ &+\frac{\eta\sqrt{\eta(1-\eta)}}{2}\left[2\hat{D}\,\hat{b}_2\hat{v}_2^\dagger + \frac{1}{2}\hat{b}_2\hat{v}_2^\dagger - 2\hat{D}\,\hat{b}_1\hat{v}_1^\dagger + \frac{1}{2}\hat{b}_1\hat{v}_1^\dagger\right]\\ &+\frac{(1-\eta)\sqrt{\eta(1-\eta)}}{4}\left[\left(2\hat{N}_{v_2} - \mathbb{1}\right)\hat{b}_2\hat{v}_2^\dagger + \left(2\hat{N}_{v_1} - \mathbb{1}\right)\hat{b}_1\hat{v}_1^\dagger\right]\end{aligned} \tag{18}$$

III. EXPECTATION VALUES OF $\hat{D}^2$ AND $\hat{D}_\eta^2$

III.1. Lossless case

With twin Fock states

$$\hat{J}_y^2 = \frac{1}{4}\left[\hat{N}_{a_1}\left(\mathbb{1} + \hat{N}_{a_2}\right) + \hat{N}_{a_2}\left(\mathbb{1} + \hat{N}_{a_1}\right) - (\hat{a}_1^\dagger)^2\,\hat{a}_2^2 - (\hat{a}_2^\dagger)^2\,\hat{a}_1^2\right] \tag{19}$$

thus with (13) (14) and (16),

$$\left\langle\hat{D}^2\right\rangle_{\text{tf}} = \left\langle\hat{J}_y^2\right\rangle_{\text{tf}}\sin^2(\phi) = \frac{N}{4}\left(1 + \frac{N}{2}\right)\sin^2(\phi) \tag{20}$$

With two-mode squeezed vacuum states

We can check that

$$m \neq n \Rightarrow \left\langle n, n\middle|\hat{D}^2\middle|m, m\right\rangle = 0 \tag{21}$$

therefore assuring the simple relation:

$$\left\langle\hat{D}^2\right\rangle_{\text{tms}} = \sum_{n=0}^{\infty} P_{th}(n)\left\langle\hat{D}^2\right\rangle_{\text{tf}} \tag{22}$$

leading to

$$\left\langle\hat{D}^2\right\rangle_{\text{tms}} = \frac{N}{2}\left(1 + \frac{N}{2}\right)\sin^2(\phi) = 2\left\langle\hat{D}^2\right\rangle_{\text{tf}} \tag{23}$$

III.2. Lossy case (i.e. eq. (8) in the main paper)

With twin Fock states

Using eq. (18), and writing the non-vanishing terms only, we have:

$$\left\langle\hat{D}_\eta^2\right\rangle_{\text{tf}} = \eta^2\left\langle\hat{D}^2\right\rangle_{\text{tf}} + \frac{\eta(1-\eta)}{4}N \tag{24}$$

therefore

$$\left\langle\hat{D}_\eta^2\right\rangle_{\text{tf}} = \eta^2\frac{N}{4}\left(1 + \frac{N}{2}\right)\sin^2(\phi) + \frac{\eta(1-\eta)}{4}N \tag{25}$$

With two-mode squeezed vacuum states

Again we can check on eq. (18) that

$$m \neq n \Rightarrow \left\langle n,n\middle|\hat{D}_\eta^2\middle|m,m\right\rangle = 0 \tag{26}$$

thus we still have

$$\left\langle \hat{D}_\eta^2 \right\rangle_{\text{tms}} = \sum_{n=0}^{\infty} P_{th}(n) \left\langle \hat{D}_\eta^2 \right\rangle_{\text{tf}} \tag{27}$$

and finally:

$$\left\langle \hat{D}_\eta^2 \right\rangle_{\text{tms}} = \eta^2 \frac{N}{2}\left(1+\frac{N}{2}\right)\sin^2(\phi) + \frac{\eta(1-\eta)}{4}N \tag{28}$$

IV. EXPECTATION VALUES OF $\hat{D}^4$ AND $\hat{D}_\eta^4$

IV.1. Lossless case

With twin Fock states

We compute $\left\langle \hat{D}^4 \right\rangle_{\text{tf}} = \left\| \hat{D}^2 \left| \frac{N}{2}, \frac{N}{2} \right\rangle \right\|^2$. The only non-vanishing term of $\hat{D}^2 \left| n,n \right\rangle$ are:

$$\begin{cases} \hat{J}_y^2 \left| n,n \right\rangle &= \frac{1}{4}\left(2n\left(1+n\right)\left|n,n\right\rangle - \sqrt{\left(n-1\right)n\left(n+1\right)\left(n+2\right)}\left[\left|n+2,n-2\right\rangle + \left|n-2,n+2\right\rangle\right]\right) \\ \hat{J}_x \left| n,n \right\rangle &= \frac{1}{2}\sqrt{n(n+1)}\left(\left|n+1,n-1\right\rangle + \left|n-1,n+1\right\rangle\right) \end{cases} \tag{29}$$

all these vectors are mutually orthogonal, then:

$$\left\| \hat{D}^2 \left| \frac{N}{2}, \frac{N}{2} \right\rangle \right\|^2 = \frac{N}{4}\left(1+\frac{N}{2}\right)\sin^2(\phi)\left[1+\frac{3}{2}\left(-1+\frac{N}{4}+\frac{N^2}{8}\right)\sin^2(\phi)\right] \tag{30}$$

With two-mode squeezed vacuum states

Looking at eq. (29), we can convince ourselves that the decomposition in the two-mode Fock basis of $\hat{J}_y^2 \left| n,n \right\rangle$ and $\hat{J}_x \left| n,n \right\rangle$ with $n \in \mathbb{N}$ generate vectors that are all mutually orthogonal.

Therefore

$$\left\| \hat{D}^2 \left| \text{TMS} \right\rangle \right\|^2 = \sum_{n=0}^{\infty} P_{th}(n) \left\| \hat{D}^2 \left| n,n \right\rangle \right\|^2 \tag{31}$$

and thus,

$$\left\| \hat{D}^2 \left| \text{TMS} \right\rangle \right\|^2 = \frac{N}{2}\left(1+\frac{N}{2}\right)\sin^2(\phi)\left[1+\frac{9N}{2}\left(1+\frac{N}{2}\right)\sin^2(\phi)\right] \tag{32}$$

IV.2. Lossy case

We follow the same procedure as before, but here the number of non-vanishing terms is much larger. We will only write the final results.

With twin Fock states

With

$$\begin{cases} P_0^{\mathrm{tf}}(N,\eta) & = 64 - 320\,\eta + 256\,\eta N + 384\,\eta^2 - 384\,\eta^2 N + 96\,\eta^2 N^2 - 144\,\eta^3 + 156\,\eta^3 N - 60\,\eta^3 N^2 + 9\,\eta^3 N^3 \\ P_1^{\mathrm{tf}}(N,\eta) & = -4\,(N+2)\,\eta\left(16 + 24\,(N-2)\,\eta + 3\left(8 - 6N + N^2\right)\eta^2\right) \\ P_2^{\mathrm{tf}}(N,\eta) & = 3\left(-16 - 4N + 4N^2 + N^3\right)\eta^3 \end{cases} \tag{33}$$

we have:

$$\left\| \hat{D}_\eta^2 \left| \frac{N}{2}, \frac{N}{2} \right\rangle \right\|^2 = \frac{\eta N}{1024}\left[P_0^{\mathrm{tf}}(N,\eta) + P_1^{\mathrm{tf}}(N,\eta)\cos(2\phi) + P_2^{\mathrm{tf}}(N,\eta)\cos(4\phi) \right] \tag{34}$$

With two-mode squeezed vacuum states

With

$$\begin{cases} P_0^{\mathrm{tms}}(N,\eta) & = 8 + 24\,\eta + 64\,\eta N + 48\,\eta^2 N + 72\,\eta^2 N^2 + 12\,\eta^3 N + 36\,\eta^3 N^2 + 27\,\eta^3 N^3 \\ P_1^{\mathrm{tms}}(N,\eta) & = -4\,(N+2)\,\eta\left(4 + 18\,\eta N + 9\,\eta^2 N^2\right) \\ P_2^{\mathrm{tms}}(N,\eta) & = 9N\,(N+2)^2\,\eta^3 \end{cases} \tag{35}$$

we have:

$$\left\| \hat{D}_\eta^2 \left| \mathrm{TMS} \right\rangle^2 \right\| = \frac{\eta N}{128}\left[P_0^{\mathrm{tms}}(N,\eta) + P_1^{\mathrm{tms}}(N,\eta)\cos(2\phi) + P_2^{\mathrm{tms}}(N,\eta)\cos(4\phi) \right] \tag{36}$$

V. PHASE UNCERTAINTY $\Delta\phi$

Phase uncertainties are computing using

$$\Delta\phi = \frac{\sqrt{\mathrm{Var}\left[\hat{D}_\eta^2\right]}}{\left| \dfrac{\partial}{\partial\phi}\left[\left\langle \hat{D}_\eta^2 \right\rangle\right] \right|}. \tag{37}$$

V.1. Lossless case (i.e. eq. (10) in the main paper)

With twin Fock states

Injecting (20) and (30) into eq. (37), we get:

$$\Delta\phi_{\mathrm{tf}} = \frac{1}{\cos(\phi)\sqrt{N(N+2)}}\sqrt{2 + \left(-3 + \frac{N}{4} + \frac{N^2}{8}\right)\sin^2(\phi)} \tag{38}$$

With two-mode squeezed vacuum states

Injecting (23) and (32) into eq. (37), we get:

$$\Delta\phi_{\mathrm{tms}} = \frac{1}{\cos(\phi)\sqrt{N(N+2)}}\sqrt{1 + 2N(N+2)\sin^2(\phi)} \tag{39}$$

V.2. Lossy case

With twin Fock states

Injecting (24) and (34) into eq. (37), we get:

$$\begin{cases} Q_0^{\mathrm{tf}}(N,\eta) & = -144\eta^3 + 384\eta^2 - 320\eta + 3\eta^3N^3 - 52\eta^3N^2 + 64\eta^2N^2 + 132\eta^3N - 320\eta^2N + 192\eta N + 64 \\ Q_1^{\mathrm{tf}}(N,\eta) & = -4\eta\,(N+2)\left(\eta^2\left(N^2 - 14N + 24\right) + 16\eta\,(N-3) + 16\right) \\ Q_2^{\mathrm{tf}}(N,\eta) & = \eta^3\left(N^3 + 4N^2 - 20N - 48\right) \end{cases} \tag{40}$$

$$\Delta\phi_{\mathrm{tf}} = \frac{1}{4N(N+2)\,\eta^2\,|\sin(2\phi)|}\sqrt{\eta\,N\left[Q_0^{\mathrm{tf}}(N,\eta) + Q_1^{\mathrm{tf}}(N,\eta)\cos(2\phi) + Q_2^{\mathrm{tf}}(N,\eta)\cos(4\phi)\right]} \tag{41}$$

With two-mode squeezed vacuum states

Injecting (28) and (36) into eq. (37), we get:

$$\begin{cases} Q_0^{\mathrm{tms}}(N,\eta) & = 3\eta + 3\eta^3N^3 + 4\eta^3N^2 + 8\eta^2N^2 + \eta^3N + 6\eta^2N + 7\eta N + 1 \\ Q_1^{\mathrm{tms}}(N,\eta) & = -2\eta\,(N+2)\left(2\eta^2N^2 + 4\eta N + 1\right) \\ Q_2^{\mathrm{tms}}(N,\eta) & = \eta^3N(N+2)^2 \end{cases} \tag{42}$$

$$\Delta\phi_{\mathrm{tms}} = \frac{1}{N(N+2)\,\eta^2\,|\sin(2\phi)|}\sqrt{\eta\,N\left[Q_0^{\mathrm{tms}}(N,\eta) + Q_1^{\mathrm{tms}}(N,\eta)\cos(2\phi) + Q_2^{\mathrm{tms}}(N,\eta)\cos(4\phi)\right]} \tag{43}$$

VI. OPTIMAL PHASE ϕ_0

When considering non-unit quantum efficiency, the phase uncertainty exhibits a minimum in $\phi_0 > 0$. In that case, the study of the derivative of $\Delta\phi$ as a function of ϕ gives the analytic expression of ϕ_0.

With twin Fock states

with $n = \frac{N}{2}$:

$$A = (1-\eta)\Big(4\eta^2\left(10n^2 - 19n + 6\right) - 2\eta^5n\left(2n^3 - 15n^2 + 24n - 9\right) - 2\eta^4n\left(-2n^3 + 31n^2 - 72n + 45\right) \\ -\eta^3\left(-33n^3 + 134n^2 - 135n + 18\right) - \eta(9 - 12n) + 1\Big)$$

we have

$$\phi_0 = \operatorname{arccsc}\left(\sqrt{\frac{\sqrt{A} + \eta^3(4n-6) + \eta^2(12-8n) + \eta(4n-7) + 1}{(1-\eta)\,(1 + \eta(4n-6)(1-\eta))}}\right) \tag{44}$$

With two-mode squeezed vacuum states

with $\nu = \frac{N}{2}$:

$$B = (1-\eta)\Big(-20\eta^5\nu^2\left(32\nu^2 + 32\nu + 5\right) - \eta^4\left(340\nu^2 - 640\nu^4\right) + 4\eta^3\nu\left(176\nu^2 + 81\nu - 15\right) \\ +4\eta^2\nu(61\nu + 26) + 7\eta(4\nu + 1) + 1\Big)$$

we have

$$\phi_0 = \operatorname{arccsc}\left(\sqrt{\frac{\sqrt{B} + 10\eta^3\nu - 20\eta^2\nu + \eta(10\nu - 1) + 1}{(1-\eta)\left(-10\eta^2\nu + 10\eta\nu + 1\right)}}\right) \tag{45}$$

Brief comment about the phase uncertainty $\Delta\phi_0$

By definition of ϕ_0, the minimal phase uncertainty $\Delta\phi_0$ is given by $\Delta\phi\Big|_{\phi=\phi_0}$. We will not give its full expression here, because it is rather long. It is simply obtained by injecting (44) and (45) into eq. (41) and eq. (43) respectively. However we have implemented it in our Python package `qsipy`.

In order to find the asymptotic limit of $\Delta\phi_0$ (i.e. eq. (11) and (13) of the main article), one must study the asymptotic expansion of the different terms of $\Delta\phi_0$. In particular, one finds that the expression of $\Delta\phi_0$ involves $\cos[2\,\mathrm{arcsec}(\bullet)]$ and $\cos[4\,\mathrm{arcsec}(\bullet)]$ terms, that must be expanded up to the second order to find the asymptotic limit.